SLAC – PUB – 4682
July 1988
(E)

DETERMINATION OF M_Z AND Γ_Z FROM THE TOTAL HADRONIC CROSS SECTION*

W. DE BOER

Max-Planck-Institut für Physik und Astrophysik,
Werner-Heisenberg-Institut für Physik, D 8000 Munich 40, Germany
and
Stanford Linear Accelerator Center
Stanford University, Stanford, California 94309, USA

ABSTRACT

We discuss the determination of the Z^0 mass and width from the total hadronic cross section with emphasis on radiative corrections and normalization errors. We find that a combined fit of the mass and width, which takes the absolute normalization of the cross section into account, significantly reduces the errors in these parameters in comparison to the standard procedure of fitting only the shape of the resonance without considering the normalization. The improvement is especially important with small data samples; at high statistics the methods become equivalent and independent of the size of the overall normalization error. From a Monte Carlo study we propose a simple scanning strategy, and also compare in detail several new Monte Carlo programs for e^+e^- annihilation including higher order radiative corrections.

Submitted to *Nuclear Instruments and Methods*

*Work supported by the Department of Energy, contract DE–AC03–76SF00515.

I. Introduction

In the near future e^+e^- collisions at the Z^0 resonance will become available and one of the first tasks will be the determination of the mass (M_Z) and width (Γ_Z) of this resonance.

The proposed extraction of M_Z and Γ_Z from the resonance shape is straightforward [1]: one just measures the μ-pair cross section as function of the center of mass energy $\sqrt{s}$ and fits the known line shape with M_Z, Γ_Z and C as free parameters:

$$\sigma_0 = \frac{C f(k,s)}{(s-M_Z^2)^2 + s^2\Gamma_Z^2/M_Z^2} \quad . \tag{1}$$

Here C is a normalization constant and $f(k,s)$ is a known radiative correction factor which depends on the fractional photon energy $k = 2E_\gamma/\sqrt{s}$. We have included explicitly the phase-space factor s^2/M_Z^2, so Γ_Z is the physical width at $\sqrt{s} = M_Z$.

However, there are two problems with this approach:

a) There is a strong correlation between the parameters, if the normalization constant C is not known. For example, C and Γ_Z are strongly correlated if $s - M_Z^2$ is small. To reduce the correlations one needs precise measurements both on- and off-resonance.

b) μ-pair final states form only 3.35% of the Z^0 final states.

In this note we study the improvements on the determination of the parameter M_Z and Γ_Z by:

- including the absolute normalization in the fit.
- including hadronic final states.

The advantage of the latter is clear: the hadronic cross section — σ_{had} — is about 90% of the visible cross section. The disadvantage is: new physics may be contributing to σ_{had}, e.g., top production or hadronic decays of a new lepton.

However, if they are contributing at a statistically significant level, it is easy to spot the new physics from specific decay signatures. On the other hand, if the contribution of the new physics is too small to detect within the given statistics, the effect on the parameters is likely to be within errors too.

Constraining the fit by the knowledge about the absolute normalization drastically improves the fit stability and parameter errors. This can be understood qualitatively as follows. Suppose one has only a few scan points in the neighborhood of the resonance (see fig. 1). If the errors are large, the shape is not well-determined. For example, the dotted line would be an acceptable fit, if only the shape is fitted. However, such a large width would give a too low absolute peak cross section, since this varies quadratically with the total width.

In sec. V we will compare quantitatively two fitting methods:

- A three-parameter fit of C, M_Z and Γ_Z to the shape of the resonance. In this case one only needs to measure the relative luminosity of the different scan points.
- If one assumes the constant C to be known from the Standard Model, one needs only a two-parameter fit of M_Z and Γ_Z to the absolute cross section, measured as function of center-of-mass energy. In this case one has to measure the absolute normalization of the scan points. C depends only on the coupling constants between the Z^0 and fermions, which are known to agree very well with the Standard Model predictions [2]. The systematic uncertainties from the luminosity monitor and the Monte Carlo acceptance corrections can cause a correlation between the different scan points. The effect of such correlations turns out to be small as will be discussed in detail.

To get the resonance shape and the absolute normalization correct, radiative corrections have to be applied. Since these corrections are sizeable, one has to include higher orders too. We have made a detailed comparison of several new Monte Carlo generators for μ-pair production, which include the higher-order corrections.

II. Standard Model Predictions

Here we summarize the formulas used in fitting the hadronic cross section. The four parameters of the $SU(3)_C \times SU(2)_L \times U(1)$ are taken to be: the fine structure constant $\alpha = 137.036^{-1}$, the Fermi coupling constant $G_F = 1.16637$ 10^{-5} GeV^{-2}, the strong coupling constant α_s and the mass of the Z^0 gauge boson M_Z. Present measurements yield for the last two parameters: $M_Z = 91.8 \pm 0.9$ GeV [3] (see fig. 2) and $\alpha_s(Q^2 = 92^2) = 0.13 \pm 0.02$ [4]. To define the couplings of the matter fields with the Z^0 it is convenient to introduce the angle $\sin^2\theta_W$, which is related to the previous parameters by:

$$\frac{G_F(1-\Delta r)M_Z^2}{8\sqrt{2}\pi\alpha} = \frac{1}{16\sin^2\theta_W\cos^2\theta_W} \quad . \tag{2}$$

Here $\Delta r \sim 0.07$ [3] is a correction term for radiative corrections, for which G_F has not yet been corrected. The main part of Δr are the $O(\alpha)$ fermion loops in the photon and weak gauge boson propagators; an additional small correction comes from the vertex and box diagrams. The loop corrections depend on the unknown top and Higgs masses; the sensitivity to the top mass becomes large if the top mass is larger than 100 GeV and present measurements of Δr require the top mass to be less than 200 GeV at the 90% C.L. [5]. The W mass can be calculated from the previous parameters:

$$M_W = \rho\, M_Z \cos\theta_W \quad . \tag{3}$$

The ρ-parameter is 1, if Higgs bosons occur only in doublets. Experimentally $\rho = 1.01 \pm 0.01$ [5], so we will assume ρ=1 in the following. The vector and axial vector couplings to the Z^0 are defined by

$$\begin{aligned} v_f &= 2(I_3^L + I_3^R) - 4\,e_f \sin^2\theta_W \\ a_f &= 2(I_3^L - I_3^R) \quad . \end{aligned} \tag{4}$$

Here I_3^L and I_3^R are the third-order components of the weak isospin. They have been summarized for the various matter fields in table 1.

With the couplings defined, the partial and total widths of the Z^0 gauge boson are found to be:

$$\Gamma_f = K r_{QCD}(v_f^2 + a_f^2) \tag{5}$$

$$\Gamma_{tot} = K\, N_g \left[a_\nu^2 + v_\nu^2 + a_e^2 + v_e^2\right] + K r_{QCD} \sum_{q=1}^{5}(v_q^2 + a_q^2) \quad . \tag{6}$$

The first part in eq. (6) is the contribution for N_g generations of leptons, while the second part sums over five quarks assuming the top quark is too heavy to contribute. The factor r_{QCD} is given in the $\overline{MS}$ scheme by

$$r_{QCD} = 3\left[1 + \frac{\alpha_s}{\pi} + 1.41\left(\frac{\alpha_s}{\pi}\right)^2 + 64.84\left(\frac{\alpha_s}{\pi}\right)^3\right] \quad . \tag{7}$$

The factor 3 on the right-hand side accounts for the color of the quarks. For $\alpha_s = 0.13$ the last two terms hardly contribute, although it should be noted that in the $\overline{MS}$ renormalization scheme the recently calculated third-order contribution is more than twice the second-order contributions [6]. The constant K can be defined as:

$$K_1 = \frac{\alpha M_Z}{48 \sin^2\theta_W \cos^2\theta_W} \tag{8}$$

or

$$K_2 = \frac{\sqrt{2} G_F M_Z^3}{48\pi} \tag{9}$$

or

$$K_3 = \frac{\alpha^* M_Z}{48 \sin^2\theta_W^* \cos^2\theta_W^*} \quad . \tag{10}$$

Here K_1 does not include the loop corrections, thus yielding the tree-level widths. K_2 can be obtained from K_1 with eq. (2), if one neglects the radiative correction factor ($\Delta r = 0$). In this case the value of K yields answers close to the complete loop calculations as pointed out by Hollik *et al.* [7]. The reason is simple:

G_F was calculated from muon decay without radiative corrections from the W-exchange graph, so G_F includes these corrections. Since the loop corrections for W- and Z^0-exchange are similar, just using K_2 in calculating the width yields answers very close to the exact answer. K_3 uses the running couplings where all loop corrections are absorbed in the Q^2-dependent coupling constants. The "starred" (= running) couplings were calculated by Lynn *et al.* [8] by summing the loop corrections to all orders. At low energies $K_3 = K_1$, while at the Z^0 energies $K_3 \sim K_2$.

From eqs. (5) and (6) it is clear that the branching ratios Γ_f/Γ_{tot} are independent of the parameterization of K and they are completely specified once $\sin^2\theta_W$ is known and the number of generations is known. For the world average [2–5] of $\sin^2\theta_W = 0.230 \pm 0.005$ one finds for three generations (and excluding the top quark contribution):

$$\frac{\Gamma_{\ell\ell}}{\Gamma_{tot}} = 3.35 \pm 0.01\% \tag{11}$$

$$\frac{\Gamma_{\nu\nu}}{\Gamma_{tot}} = 6.65 \,{}^{+\,0.04}_{-\,0.03}\% \tag{12}$$

$$\frac{\Gamma_{qq}}{\Gamma_{tot}} = 70.00 \pm 0.12\% \quad . \tag{13}$$

The total hadronic cross section is given by:

$$\sigma^{\gamma}_{had} = \frac{4\pi\alpha^{*2} r_{QCD}}{3s} \sum_{q=1}^{5} e_e^2 e_q^2 \tag{14a}$$

$$\sigma^{\gamma Z}_{had} = \frac{8\pi\alpha^{*} K r_{QCD}}{M_Z} \; \frac{(s - M_Z^2) \sum_{q=1}^{5} e_e e_q v_e v_q}{(s - M_Z^2)^2 + s^2\Gamma_{tot}^2/M_Z^2} \tag{14b}$$

$$\sigma^{Z}_{had} = \frac{12\,\pi r_{QCD}}{M_Z^2} \; \frac{s\,K^2(v_e^2 + a_e^2) \sum_{q=1}^{5} (v_q^2 + a_q^2)}{(s - M_Z^2)^2 + s^2\Gamma_{tot}^2/M_Z^2} \quad . \tag{14c}$$

The superscripts indicate the contribution from photon exchange, Z^0 exchange and their interference and K is one of the K's defined in eqs. (8)–(10). The sum is taken over five quark flavors, thus assuming the top quark is too heavy. Combining eqs. (5) and (14c) one finds the important result that on resonance, when $s = M_Z^2$,

$$\sigma_{had}^{peak} = \frac{12\pi}{M_Z^2} \frac{\Gamma_{ee}\Gamma_{qq}}{\Gamma_{tot}^2} \tag{15}$$

is independent of K and thus largely independent of uncertainties in the loop corrections coming from the unknown top and Higgs masses.

Choice of K-factor

The parameters describing the total cross section in eq. (14) are: α, α_s, M_Z, Γ_Z, e_e, e_q,v_e, v_q, a_e a_q and, in addition, G_F or $\sin^2\theta_W$ depending on the choice of K-factor [eqs. (8)–(10)]. The most unknown and most interesting parameters are M_Z and Γ_Z, so one can try to optimize the knowledge on these parameters by taking the other parameter values from independent processes. For example, α, e_e, e_q, a_e and a_q are well-known; v_e and v_q are reasonably well-known from eq. (4) and the world average of $\sin^2\theta_W$ and the uncertainty of 0.02 in α_s yields an uncertainty in the peak cross section of 0.4% only. The remaining choice to be made is the K-factor. Experimentally, K_2 is most accurately known and therefore preferred. Furthermore, by using K_2 the radiative corrections are smaller and easier to handle. First of all, because the width calculated with K_2 is very close to the width calculated with the complete radiative corrections. Therefore, the shape is correctly described and the initial-state radiative corrections, which are rather sensitive to the shape, can be calculated in a straightforward way. Secondly, the electroweak loop corrections are small, if one uses K_2, since K_2 and K_3 are almost identical in the Z^0 resonance region.

If one uses K_3 or K_1 instead of K_2, one can in principle fit $\sin^2\theta_W$ as an additional free parameter [the dependence of the cross section on this parameter is now much stronger than the dependence via the vector couplings alone as

given by eq. (4)]. One can then make a test of the Standard Model by comparing this value of $\sin^2\theta_W$ with the world average. An alternative test would be to determine M_Z using K_2, insert its value into eq. (2) and compare the left- and right-hand sides in eq. (2). However, these tests are model-dependent in the sense that they depend on the unknown top and Higgs masses: in case of K_1 one has to apply the radiative corrections to the data, in case of K_3 one has to calculate K_3 for a certain top and Higgs mass and in case of K_2 one has to calculate Δr in eq. (2). In the fits described in sec. V we have used the parametrization with G_F (K_2).

The total cross section

From eqs. (11), (13) and (15) the hadronic peak cross section is found to be 40.7 nb at the Born level. The observable peak cross section after radiative corrections is $0.736 \times 40.7 = 30.0$ nb (see next section). This cross section depends quadratically on the total width and is therefore sensitive to the number of neutrino species with masses less than half the Z^0 mass. If one expresses Γ_{ee} and Γ_{qq} as fractions of the total width [see eqs. (11) and (13)], one finds for the contribution of N_ν^{new} new neutrinos:

$$\sigma_{had}^{peak} = \frac{12\,\pi}{M^2}\,\frac{(0.0335)\,(0.700)}{(1+0.0665\,N_\nu^{new})^2} \quad . \tag{16}$$

One new neutrino generation will lower the peak cross section by 12.7% independent of m_t and m_H and this should not be too difficult to detect: with a 5% statistical error (implying 400 observed Z^0 events) and a 5% systematic uncertainty, the one-sided 90% C. L. lower limit would be 11.5%, which is still below the change expected for one new neutrino generation. Here we assumed that the mass of the new neutrino is at least a few GeV below half the Z^0 mass. More quantitative results on the total error of Γ_{tot} will be given in sec. V.

III. Radiative Corrections

In order to measure either the shape or the absolute cross section, one has to apply radiative corrections. For hadronic final states these reduce to

- Initial state radiation from the electrons. Final-state electromagnetic radiation from the quarks is small since

  a) The Kinoshito-Lee-Nauenberg theorem assures that the procedure of summing over all $q\bar{q}$ final states with an arbitrary number of photons, as is done in the detection of multihadronic events, will cancel all leading logarithms and the remaining radiative correction is of order $O\left(\frac{\alpha}{\pi}\right) \approx 0.2\%$.

  b) Fragmentation of quarks (strong interactions) is fast compared to the timescale of electromagnetic radiation.

- Loop corrections to the gauge boson propagators, which are called vacuum polarization corrections in case of the photon and "oblique" corrections in case of the weak gauge bosons. These loops depend on the maximum Q^2 of the gauge boson and can be taken into account by either modifying the coupling constants ("running" coupling constants) or by correcting the propagators. The size of the loop corrections depends strongly on energy: at $s = M_Z^2$ the effect is small, since the K-factors largely cancel out [see eq. (15)]. Off-resonance, where $(s - M_Z^2)^2 \gg M_Z^2\Gamma_Z^2$, the radiative corrections are K_3^2/K_1^2. This factor is approximately 1.14 at $\sqrt{s} = 80$ GeV, where 12.6% comes from the running of α and the remaining part comes from vertex and box diagrams.

The size of initial state radiative corrections is shown in table 2; the factors were calculated with different Monte Carlo generators and from the formulas of ref. [9] with the program ZAPPR from G. Burgers. The Born cross section has to be multiplied by these factors in order to obtain the corrected cross section. The minimum allowed invariant mass squared of the final state — s′ —

was taken to be 1% of s in all calculations. It can be seen that the first-order corrections change the Born cross sections by factors between 1.9 and 0.7; for such large corrections the higher-order corrections are important. Until recently these higher-order corrections had been estimated by an approximate procedure, called "exponentiation;" recently Berends, Burgers and van Neerven [9] showed that these estimates are very close to the exact second-order calculation. Several new Monte Carlo generators have become available, which include higher-order, initial-state radiative corrections as well as the loop corrections. An overview is given in table 3. The ones of interest to hadron production are:

- MMGE. This is the original Berends-Kleiss-Jadach [10] μ-pair generator updated by J. Alexander [11] with the second order calculations of ref. [9]. The program has various options:

  Calculate first- (second-) order initial-state radiation with at most one (two) photon(s) from initial-state radiation.

  Exponentiate the cross sections to include the effects of multiple soft photon emissions (both first and second order). The program does not include the loop corrections.

- YFS. This program from Jadach and Ward [12] follows the exponentiation procedure from Yennie, Frautschi and Suura [13]. It is unique in the sense that it calculates higher-order initial state radiation with multiple photons generated as real particles, thus taking correctly the kinematics of multiple photons into account including a non-zero invariant mass. In the previous program MMGE only the remaining energy after radiation was calculated and the missing energy was attributed to a single effective, massless photon.

- EXPOSTAR. This program, developed by Im, Kennedy, Lynn and Stuart [8], takes all the loop corrections into account by calculating the running couplings. Higher-order, initial-state radiative corrections are taken into account via the structure function approach [14], in which the longitudinal momenta of the electron or positron are partially transferred

to photons. Since these photons cannot have transverse momenta, the program is not suitable as a Monte Carlo generator, but it is very useful to check total cross sections and radiative correction factors. In the program BREM6 these transverse components will be reinstated by combining the original Berend-Kleiss-Jadach generator (BREM5) with EXPOSTAR. However, BREM6 has not yet been released.

Figure 3 shows the effect of higher-order contributions to the differential cross section $d\sigma/dv$. Here $v = 1 - s'/s$, where s and s' are the invariant masses squared of the initial and final state, respectively. In first order v would just be the fractional photon energy $E_\gamma/E_{\rm beam}$. In second order one cannot speak about the photon energy, but s' is still a well-defined quantity. One observes that higher order contributions shift the events towards larger v, as expected since larger v corresponds to smaller s' and more initial state radiation reduces s'.

Figure 4 shows the ratio between the second order and first order differential cross section. One observes a large decrease (20–30%) in the region of soft real photons ($v \to 0$), which is only partially compensated by an increase of approximately 10% in the region of hard photon radiation (large v). The fact that the total cross section still increases by 0.8% is due to the increase in the infrared part of the cross section.

In fig. 5 we compare the differential distributions $d\sigma/dv$ for the MMGE and YFS Monte Carlo generator with the analytical formula of ref. [9] by plotting the Monte Carlo events and weighting each entry with the inverse of the analytical formula, so one expects a straight line close to 1.

One sees that both programs agree well with the analytical formulae. For YFS we plotted the results for two values of the maximum allowed energy of the photons, which can be radiated in addition to the first photon. One sees that the contribution from two or more hard photons is appreciable.

At energies above the Z^0 mass both the YFS and MMGE programs deviate appreciably from the results of the EXPOSTAR program. This is due to the fact that the latter program includes the loop corrections, which cause a larger width of the resonance (EXPOSTAR calculates the width with K_3, while the other programs use K_1). Simply inserting a larger width in the other programs will make the radiative correction factors to become similar, but then the peak cross section will be wrong. One has to include correctly the running of the coupling constants, since even approximating K_3 with K_2 does not yield the correct answer as seen from the comparison of $f_{EXPO}^{K_3}$ and $f_{2E}^{K_2}$ in table 2, although the difference is less than 1%.

In table 2 we have also included a column with the total cross section for μ-pair production after all radiative corrections. The cross section for the other channels can be calculated from the relative branching ratios [see eqs. (11)–(13)] and the relative contributions of photon and Z^0 exchange [see eq. (14)]. The absolute cross section in table 2 is in good agreement with the result calculated from the experimental branching ratios [eqs. (11)–(13)] only if we apply the weak vertex corrections consistently to both the running coupling constants in eq. (14) and the width. This was not done in EXPOSTAR and ref. [8], so the peak cross section is lower in that case by about 20 pb compared to the value in table 2, but is closer to a recent calculation by G. Burgers [15] (10 pb lower).

IV. Fitting Method for Correlated Errors

The best estimates of M_Z and Γ_Z can be extracted from the data via a fitting procedure, e.g., minimizing the χ^2 [16]. Correlated errors between measurements can be taken into account in one of the following ways [17]:

a) Define the χ^2 via an error correlation matrix:

$$\chi^2 = \Delta^T V^{-1} \Delta \quad . \tag{17}$$

Here Δ is a column vector containing the residuals between measurements (R_i) and fitted values (R_{fit}) and V is the error correlation matrix:

$$\Delta_i \;=\; R_i - R_{fit}$$

$$V_{ii} \;=\; E(R_i - R_{fit})^2 \;=\; \sigma_i^2 \;+\; \sigma_n^2 \qquad (18)$$

$$V_{ij} \;=\; E(R_i - R_{fit})(R_j - R_{fit}) \;=\; \sigma_n^2 \quad .$$

E indicates that the expectation value has to be calculated, σ_i is the error on R_i and σ_n is the overall normalization error, which indicates how far the observed value(R_i) can deviate from the true value (R_t), so $R_i = R_t \pm \sigma_n$. This last expression inserted in the expectation values in eq. (18) yields the results for the elements of V. Note that σ_i^2 is the variance of R_t, so it contains the uncorrelated part of the error, which includes both the statistical error and point-to-point systematic error, but excludes the overall normalization error. For example, for two measurements R_1 and R_2 with statistical errors of 10% and a normalization error of 5%, the matrix is:

$$V = \begin{pmatrix} (0.1\,R_1)^2 + (0.05\,R_1)^2 & (0.05\,R_1 R_2)^2 \\ (0.05\,R_1 R_2)^2 & (0.1\,R_2)^2 + (0.05\,R_2)^2 \end{pmatrix} \quad .$$

The following points are worthwhile noting:

- This error matrix is $N \times N$ for N data points and should not be confused with the $M \times M$ error matrix for M fitted parameters: the first matrix is input to the fit program, the second one output.
- The importance of systematic errors can be studied by varying the off-diagonal elements and observing the influence on the fitted parameters.

b) A second method commonly used to take correlated errors into account is the following: Define a likelihood function by multiplying the probability of each data point with the common probability factor from the overall normalization factor f, which is assumed to have a Gaussian distribution with mean 1 and r.m.s. σ_n:

$$\mathcal{L} = \sum_{i=1}^{N} e^{-\left(\frac{f-1}{\sigma_n}\right)^2} e^{-\frac{(fR_i - R_{fit})^2}{(f\sigma_i)^2}} \quad . \tag{19}$$

For small event samples the Gaussian event error distribution can be replaced by a Poisson distribution.

One can optimize the likelihood by minimizing

$$\chi^2 = \left(\frac{f-1}{\sigma_n}\right)^2 + \sum_{i=1}^{N} \frac{(fR_i - R_{fit})^2}{(f\sigma_i)^2} \quad . \tag{20}$$

f can either be treated as a free parameter or one integrates over all possible f values in the fit.

Methods a) and b) usually give similar results. However, the first method is more flexible in the sense that it defines a correlation between every pair of data points and it does not require a specific error probability distribution as is needed in case of the maximum likelihood approach. Therefore we will use the first method.

V. Monte Carlo Fit Results

Before generating MC events one has to decide the number of scan points and the distance Δ between the scan points. To fit eq. (1) to the shape, one needs at least three scan points. If one measures the averaged energy for each event, one could have as many energy points as events. This can be easily included in the fit of the data as a function of energy, but for the moment we will assume that we have the equivalent of three data points at three energies separated by a distance Δ. Data point at more energies can only improve the fit, so the results present a pessimistic limit.

Since the mass of the Z^0 is not known accurately, one may miss the peak by some amount. We therefore generated Monte Carlo events in three energy bins each Δ GeV apart and assumed the central point misses the peak by ϵ GeV, so $\epsilon = < \sqrt{s} > - M_Z$.

We generated the events first as function of ϵ for different values of Δ, then as function of Δ for different values of ϵ. Figures 6 and 7 show some typical fit results for M_Z and Γ_Z as function of ϵ for $\Delta = 1.5$ and 1 GeV, respectively. Each error bar corresponds to a fit for a total luminosity of 3.3 nb^{-1} divided equally over three scan points. If the points were centered around the peak, i.e., $\epsilon = 0$, this corresponds approximately to

33 events at 92 GeV,
25 events at 93 GeV, and
22 events at 91 GeV.

One sees from figs. 6 and 7 that the fitted values of M_Z and Γ_Z cluster around the generated values of 92 and 2.55 GeV, respectively, even if $\epsilon = \pm 1$ GeV. For these values of ϵ and $\Delta = 1$ GeV one measures only on one side of the resonance (see the insets in figs. 6a and 7a for scan point positions for $\epsilon = 1$, 0, and –1 GeV). In this case the correlation between M_Z and Γ_Z becomes large as shown in fig. 7c, top and bottom. As soon as one measures on both sides of the peak, the correlation becomes reasonably small even if $\epsilon = \pm 1$GeV (see fig. 6c).

Typical errors are 200–350 MeV, both for M_Z and Γ_Z. Here we assumed that the luminosity was measured with a total systematic uncertainty of 15%, which we assumed to be fully correlated between the data points. The statistical error on the luminosity was assumed to be small compared with the systematic error and therefore neglected. The effect of larger systematic errors will be discussed hereafter.

Figures 8 to 10 show the typical error on M_Z and Γ_Z as function of the scan range (defined as 2Δ) for $\epsilon = 0$, 0.5, and 1 GeV, respectively. The two lower curves show the correlations between M_Z and Γ_Z and the number of events normalized to the total number of "peak" events N_t, where N_t is the number of events expected if all the luminosity was taken at the peak of the resonance. This ratio decreases if the scan range increases since the luminosity was kept constant. The different symbols correspond to different values of "peak" events. If one measures symmetrically around the peak ($\epsilon = 0$, fig. 8), the correlation ρ is small and the smallest errors are obtained for a small scan range, thus optimizing the number of events. If the central point misses the peak by 0.5 or 1.0 GeV the smallest error in M_Z is obtained for a larger scan range (see figs. 9 and 10), while the smallest error in Γ_Z is obtained for the scan range optimizing the number of events.

Figure 11 shows the dependence of the expected error in Γ_Z on the scan range for different mixtures of statistical and normalization errors. One sees that for a luminosity corresponding to 100 "peak" events the results from a two parameter fit (M_Z and Γ_Z) gives a considerably better result than a three parameter shape fit in which the the normalization constant is an additional free parameter. This holds even for very large statistics (10^5 Z^0's) and large normalization errors; the two parameter fit results shown have normalization errors of 3, 15 and 25%, respectively.

With high statistics and a sufficiently large scan range all fits become similar and independent of the normalization error (see fig. 11, top curve). The reason is

simple: M_Z is best determined by points on the steeper slope of the resonance, while Γ_Z is most sensitive to the peak cross section, where the term $(s - M_Z^2)$ is small. One cannot determine one parameter precisely without knowing the other, so one needs a certain minimum scan range and the most unbiased way of extracting M_Z and Γ_Z is a simultaneous fit of both parameters. If the scan range is large enough, the normalization error can move all points up and down, but this does not change the shape. In this case the shape fit and the fit of the absolute cross section become equivalent. Note that the final error on the width is determined by the point to point systematic uncertainties, which we assumed to be 1% for the curves in fig. 11. Even with 10^2 to 10^3 events one can get useful limits on the number of generations with light neutrinos (masses less than $M_Z/2$), since the errors on the total width become comparable to the contribution of a new neutrino generation, which is shown as a dashed horizontal line in fig. 11.

VI. Scanning Strategy

We assume the first data will be taken at a center-of-mass energy close to the expected Z^0 mass of 92 GeV (see fig. 2). If one takes 1 nb^{-1} ($\approx$ 30 "peak" events) and assumes the width to be equal to the predicted value of 2.55 GeV, one can calculate from eq. (14c) the relative position of the peak, namely $(s - M_Z^2)^2$. The accuracy of the peak position is about 0.4–0.7 GeV, depending on how far one misses the peak (see horizontal error bars in fig. 1). The error becomes larger at the peak, since the cross section is rather flat near the peak. In the unlikely case that one misses the peak by several GeV, the best strategy would be to find the peak and one should change the energy by the amount given by the measured $s - M_Z^2$.

Because of the quadratic ambiguity in $(s - M_Z^2)^2$, one does not know in which direction to move. We propose to move up in energy, since this has the advantage of the larger cross section from the radiative tail. We will not consider any further

the pessimistic scenario of missing the peak by several GeV, since this has been worked out before [18].

If one misses the peak by 1 GeV or less, one can see from figs. 8–10 that a reasonable scan range is 2 GeV, so a good next energy point would be 93 GeV. After having two points measured, one can solve the quadratic ambiguity in $(s - M_Z^2)^2$ and decide where to take the third point. By comparing the absolute value of the minima in figs. 8–10 one sees that the errors on M_Z and Γ_Z are almost independent of ϵ, i.e., where the scan points are located on the peak, but for every case the optimum scan range has to be choosen with some care.

VII. Summary

We have compared two ways of extracting the Z^0 mass and width from an energy scan over the resonance:

a) In the first case we made a two-parameter fit of M_Z and Γ_Z to the absolute total cross section assuming the couplings of the Z^0 to quarks and leptons to be known from the world average of the electroweak mixing angle. In this case one relies on the absolute measurement of the luminosity, which causes a correlated error between the measurements at different energies. Note that we could have used also the constraint between the mass M_Z and the coupling constants [eq. (2)], in which case the only free parameters are M_Z and Γ_Z. However, in this case one becomes model dependent, namely one has to assume something about the Higgs sector and guess some value for the top quark mass in order to calculate Δr. Therefore, we have calculated the couplings from the world average of $\sin^2\theta_W$, which is quite well-known now.

b) In the second method one fits only the shape of the resonance by using the overall normalization as an additional free parameter. Then one only has to know the relative luminosity between the measurements at

different energies and avoids the correlation from the common normalization error.

However, it turns out that the first method always gives much more stable fit results and smaller errors, even if the normalization error is large. The difference is especially important in case of low statistics: with about 10^2 events divided over three scan points and a common normalization error of 15%, the expected errors on the mass and width are as low as 0.25 GeV each. A shape fit alone would increase these errors by at least a factor of 2.

Both methods require knowledge of the radiative corrections and several new Monte Carlo generators including these corrections have been discussed. The new Monte Carlo generators were found to be in good agreement with the exact second order calculations of ref. [9]. However, a precise determination of the radiative correction factors requires taking into account the loop corrections, since these corrections do not make an overall normalization change, as often stated, but they change the shape of the resonance and therefore change the radiative correction factors. These corrections have been implemented in the EXPOSTAR program, but this program does not generate transverse momentum for the radiated photons. These loop corrections can be incorporated in the other programs easily in an approximate way, namely by defining the Born cross section and the width both with the parametrization using the Fermi constant [K_2 in eq. (9)]; this yields correction factors accurate to about 1% as shown in table 2. Higher precision requires the complete loop corrections to be implemented. With the proposed fitting procedure we have studied the errors on M_Z and Γ_Z as function of scan range and a simple scanning strategy has been discussed in the previous section in order to minimize the errors on these parameters.

ACKNOWLEDGMENTS

I gratefully acknowledge the numerous discussions on radiative corrections with Frits Berends, Gerrit Burgers, Wolfgang Hollik, Jung Im, Stascek Jadach, Dallas Kennedy, Ronald Kleiss, Mike Levi, Brian Lynn, Patricia Rankin and Bennie Ward. I also like to thank Patricia Rankin, Markus Schaad and Bennie Ward for a careful reading of the manuscript. and thank the SLAC directorate for the hospitality enjoyed during my stay at SLAC.

REFERENCES

1. For example, A. Blondel *et al.*, in Physics at LEP, CERN 86-02, p. 35.
2. W. de Boer, *Proceedings of the 17th International Symposium on Multiparticle Dynamics*, Seewinkel, Austria (1986), Ed. M. Markytan.
3. P. Langacker, W. J. Marciano and A. Sirlin, Phys. Rev. **D36** (1987) 2191.
4. W. de Boer, SLAC–PUB–4428, and *Proceedings of the 10th Warsaw Symposium on Elementary Particle Physics*, Kazimierz, Poland (1987), Ed. Z. Ajduk, p. 503.
5. U. Amaldi *et al.*, Phys. Rev. **D36** (1987) 1385.
6. S. G. Gorishny, A. L. Kataev and S. A. Larin, Preprint JINR E2-88-254 (1988).
7. W. Hollik, DESY 86-049, *Proceedings of the 21st Rencontre de Moriond*, Les Arcs, France, 1986; G. J. H. Burgers and W. Hollik, CERN-TH.5131/88. M. Böhm *et al.*, Fortsch. Phys. **34** (1986) 687.
8. D. Kennedy, B. W. Lynn, C. J. C. Im and R. G. Stuart, SLAC-PUB-4128, submitted to Nucl. Phys. B.
9. F. A. Berends, G. J. H. Burgers and W. L. van Neerven, Phys. Lett. **185B** (1987) 395. The program ZAPPR for these second-order calculations has been obtained from G. J. H. Burgers.
10. F. A. Berends, R. Kleiss and S. Jadach, Comp. Phys. Commun. **29** (1983) 185.
11. J. P. Alexander, private communication and J. P. Alexander, G. Bonvicini, P. S. Drell and R. Frey, Phys. Rev. **D37** (1988) 56.
12. S. Jadach and B. F. L. Ward, SLAC-PUB-4543, submitted to Phys. Rev. D.
13. D.R. Yennie, S.C. Frautschi and H. Suura, Annals of Phys. **13** (1961) 379.

14. O. Nicrosini and L. Trentadue, Phys., Lett. **196B** (1987) 551, FNT/T-87/17.

15. G. J. H. Burgers, CERN-TH.5119/88.

16. We used the MINUIT fit program from the CERN Program Library written by F. James and M. Roos, J. Comp. Phys. Comm. **10** (1975) 343.

17. G. D'Agostini, private communication. J. Orear, Note on statistics for physicists, Cornell preprint CLNS 82/511, p. 37. CELLO Coll., H. J. Berend et al., Phys. Lett. **138B** (1987) 400.

18. P. Rankin, Mark II/SLC—Physics Working Group Note #1-14.

Table 1. Summary of couplings for $\sin^2\theta_W = 0.23$.

Fermion	I_3^L	I_3^R	a	v	e_f
neutrino	1/2	0	1	1	0
e, μ, τ lepton	−1/2	0	−1	$-1+4\sin^2\theta_W = -0.08$	-1
u, c, t quarks	1/2	0	1	$+1-\frac{8}{3}\sin^2\theta_W = +0.39$	+2/3
d, s, b quarks	−1/2	0	−1	$-1+\frac{4}{3}\sin^2\theta_W = -0.69$	−1/3

Table 2. Initial state radiative correction factors for μ-pair production for a maximum v-value of 0.99. The superscript K refers to the K factor [see eqs. (8)–(10)] used to define the cross section, so K_1 means no loop corrections at all (also no loop corrections for the photon annihilation channel and the interference term [eqs. (14a) and (14b)]; K_3 means the complete loop corrections have been taken into account in all channels. $f_{1(e)}$ and $f_{2(e)}$ are the radiative correction factors with at most 1 and 2 photons radiated in the initial state, respectively; the subscript e indicates if the exponentiated cross sections were used; these factors were calculated with the formulas of ref. [9] using the program ZAPPR from G. Burgers. The subscripts MMGE, YFS, and EXPO indicate the programs from which these factors were calculated. σ_{EXPO} gives the absolute cross section in nanobarn for M_Z=92 GeV, a top mass of 50 GeV, a Higgs mass of 100 GeV, and a maximum v-value of 0.99. The precision of the various f's is typically 0.005 or better. The YFS program has not been run at all energies because of its appetite for computer CPU time. The following points are worth noting (see text): a)The appreciable difference between f_1 and f_{1e} in the neighborhood of the resonance; b) The small differences between f_{1e}, f_2, and f_{2e}; c) The appreciable differences between $f_{EXPO}^{K_3}$ and $f_{MMGE}^{K_1}$ at the highest energies; d) The reasonable agreement between $f_{EXPO}^{K_3}$ and $f_{2e}^{K_2}$ indicating that the loop corrections are small if K_2 is used.

$\sqrt{s}$	$f_1^{K_1}$	$f_{1e}^{K_1}$	$f_2^{K_1}$	$f_{2e}^{K_1}$	$f_{2e}^{K_2}$	$f_{MMGE}^{K_1}$	$f_{YFS}^{K_1}$	$f_{EXPO}^{K_3}$	$\sigma_{EXPO}^{K_3}$ (nb)
20	1.245	1.255	1.255	1.255	1.255	1.252	1.253	1.259	0.299
40	1.259	1.271	1.271	1.271	1.271	1.267	1.262	1.276	0.077
60	1.247	1.259	1.259	1.259	1.259	1.256	1.244	1.264	0.036
80	1.025	1.040	1.040	1.041	1.040	1.036	1.032	1.040	0.035
87	0.793	0.826	0.825	0.824	0.824	0.821	—	0.822	0.104
88	0.756	0.794	0.793	0.792	0.792	0.789	0.769	0.792	0.149
89	0.718	0.762	0.762	0.760	0.760	0.757	—	0.759	0.234
90	0.679	0.730	0.732	0.728	0.730	0.726	0.714	0.729	0.424
91	0.648	0.706	0.709	0.703	0.708	0.701	—	0.706	0.883
92	0.688	0.733	0.731	0.730	0.739	0.728	0.725	0.736	1.442
93	0.906	0.888	0.874	0.886	0.885	0.883	—	0.881	1.049
94	1.186	1.104	1.087	1.106	1.088	1.102	1.087	1.081	0.615
95	1.449	1.322	1.307	1.327	1.294	1.322	—	1.286	0.398
96	1.682	1.524	1.515	1.534	1.486	1.528	1.527	1.477	0.285
97	1.884	1.708	1.706	1.722	1.662	1.716	—	1.654	0.217

Table 3. **MC GENERATORS:** $e^+e^- \to \gamma Z^0 \to \mu^+\mu^-$.

Program	Authors	Ref.	Initial State Radiation	Final State Radiation	Loop Corr.	Pol.
MMG	F. A. Berends R. Kleiss S. Jadach	10	$0(\alpha)$	+	−	−
MMGE	J. Alexander	11	$0(\alpha^2)$ + exp.	−	−	−
BREM5	R. Kleiss B. W. Lynn R. G. Stuart	8	$0(\alpha)$	+	+	+
EXPOSTAR	C. J. C. Im D. Kennedy	8	structure functions	−	+	+
BREM6†	BREM5 EXPOSTAR	−	structure functions	+	+	+
YFS*	S. Jadach B. F. L. Ward	12	multiple photons	−	−	+
BHKMUON†	F. A. Berends W. Hollik R. Kleiss	−	$0(\alpha)$	+	+	−

† not yet released.

* A new version, together with Z. Was, will include the loop corrections.

FIGURE CAPTIONS

1. The expected number of events as function of center of mass energy for $M_Z = 92$ GeV and a luminosity of 1.1 nb^{-1} for each energy point. The vertical error barr indicates the statistical error, while the horizontal error bar indicates the expected error on M_Z, if one calculates M_Z from that single energy point assuming the width to be known.

2. A summary of the present knowledge about M_Z from the $p\bar{p}$ collider experiments UA1 and UA2, the combined neutral current data[2] ($\sin^2\theta_W$), and the rise in the hadronic cross section at PETRA and KEK (R) (calculated from the results described in ref. [4]).

3. The v–distribution in first and second order. In first order, v is the photon energy normalized to the beam energy. The solid curves were calculated from the formulae in ref. [9]. The dots were obtained from the MMGE Monte Carlo generator.

4. As in Fig. 3 but for the exponentiatied cross sections normalized to the first order cross section.

5. The v–distribution of the MMGE Monte Carlo generators MMGE (a) and YFS (b) normalized to the exact second order calculation of ref. [9]. One sees good agreement with the expected straight line. In fig. 5b we have also plotted the result, if the energy of the photons radiated in addition to the first photon is limited to 3 GeV. From the difference one sees that the contribution from two or more hard photons is appreciable. These comparisons were done at $\sqrt{s} = 60$ GeV; at this energy the contribution from hard photon radiation is large in contrast to the radiation from the Z^0 resonance, where the radiation of hard photons is negligible because of the sharpe decrease in the cross section at lower energies.

6. The fitted values of M_Z and Γ_Z and their correlation ρ as function of ϵ for three scan points separated by $\Delta = 1.5$ GeV. ϵ is the distance of the central point to the peak, so the location of the scan points on the resonance is as indicated on the left in (a) for $\epsilon = 1$, 0, and –1 GeV. Each error bar is the result of a fit to Monte Carlo generated

events with a total luminosity of 3.3 nb^{-1} equally divided over three energy scan points. This luminosity corresponds to 100 events at the peak, but only $\approx$ 80 and 60 events, if the luminosity is divided over three scan points with $\epsilon = 0$, and 1 GeV, respectively.

7. As in fig. 6, but for a smaller scan range: $\Delta = 1$ GeV. In this case the correlation between M_Z and Γ_Z becomes appreciably larger.

8. The expected error on M_Z and Γ_Z and their correlation ρ as a function of the scan range, which is defined as the difference in energy between the highest and lowest point. The lower curve shows the decrease in event numbers with increasing scan range. The three scan points were taken symmetrically around the peak ($\epsilon = 0$ GeV).

9. As fig. 8, but for $\epsilon = 0.5$ GeV.

10. As fig. 8, but for $\epsilon = 1.0$ GeV.

11. The expected error on the width for different event samples (expressed in number of "peak" events N_t) and different normalization errors (σ_n), which cause a correlation between the different energy points. The crosses indicate the error from the shape fit alone, thus disregarding the information from the absolute value of the cross section. Note that the fit using the normalization is always better than the shape fit, even in case of large normalization errors and high statistics (see text).

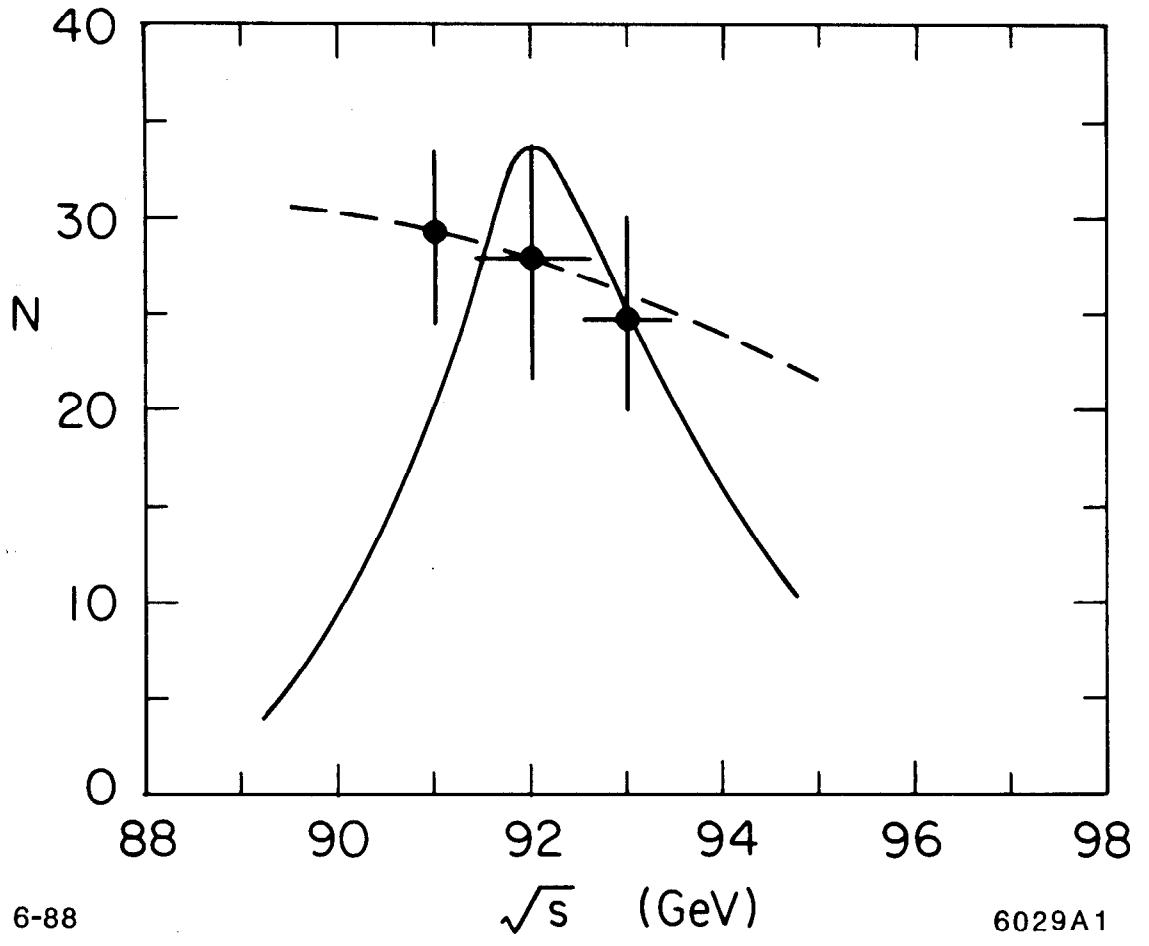

Fig. 1

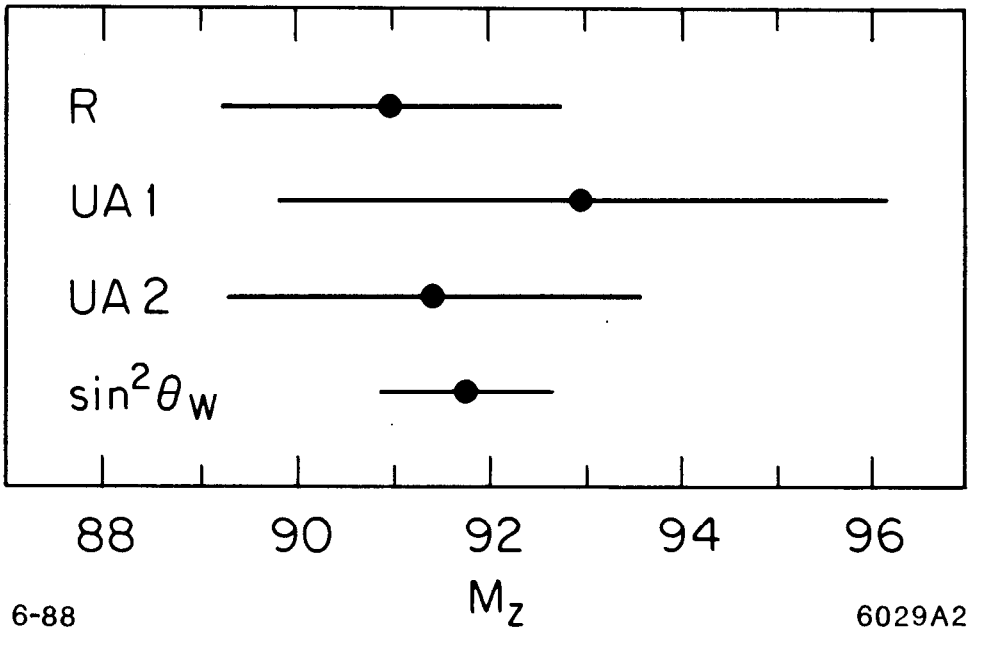

Fig. 2

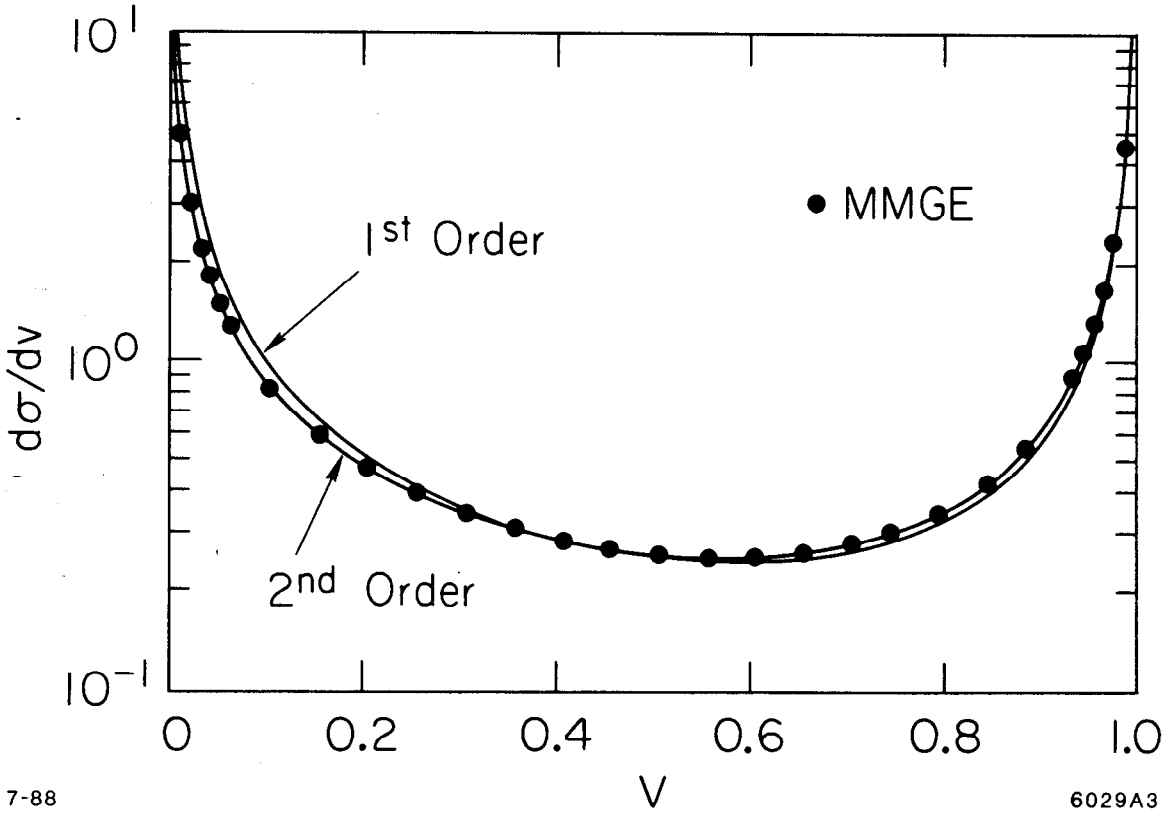
10^1
10^0
10^{-1}
dσ/dv
0
0.2
0.4
0.6
0.8
1.0
V
• MMGE
1st Order
2nd Order
7-88
6029A3

Fig. 3

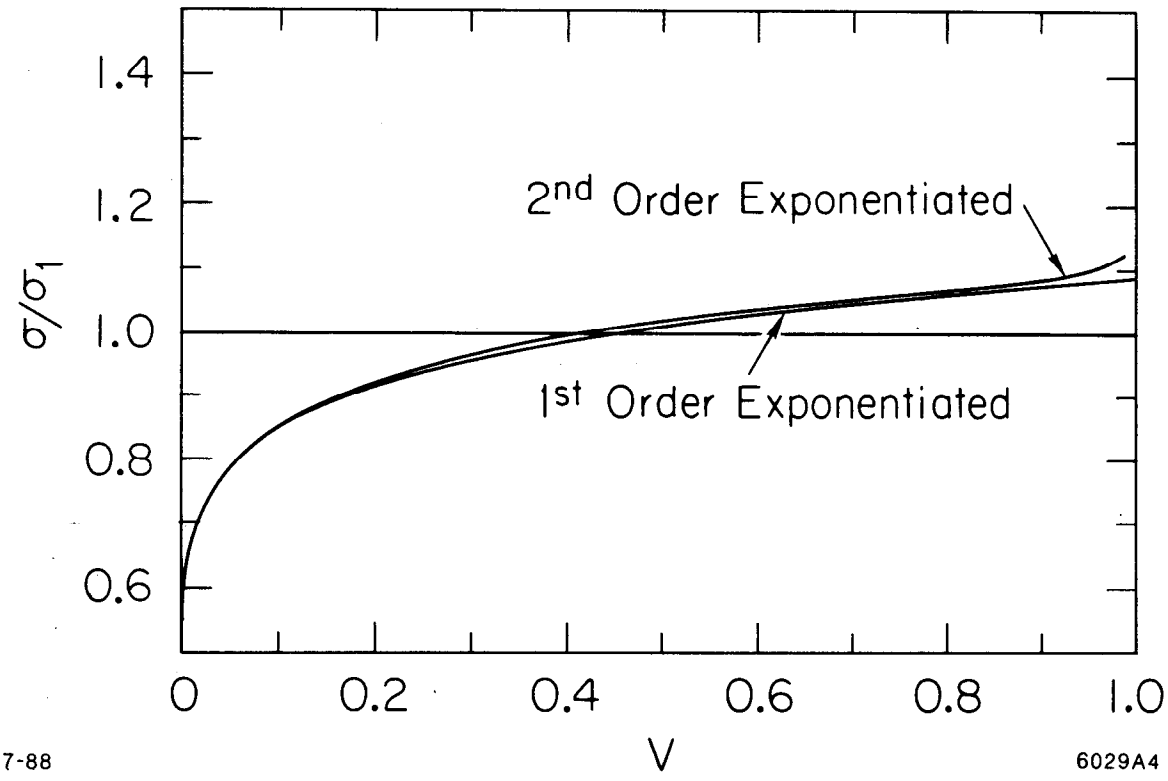
1.4
1.2
1.0
0.8
0.6
σ/σ1
2nd Order Exponentiated
1st Order Exponentiated
0
0.2
0.4
0.6
0.8
1.0
V
7-88
6029A4

Fig. 4

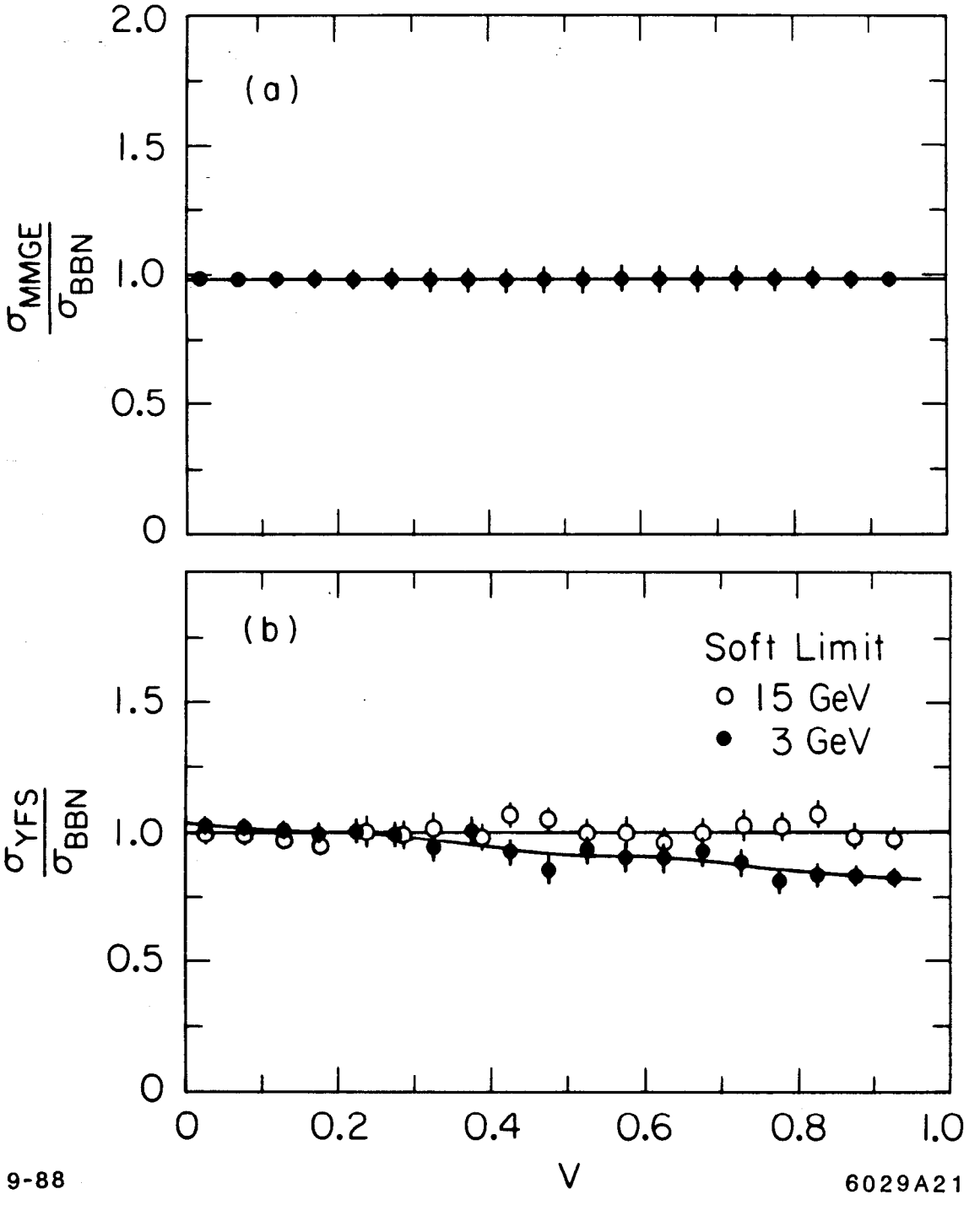
(a)
(b)
Soft Limit
15 GeV
3 GeV
$\frac{\sigma_{MMGE}}{\sigma_{BBN}}$
$\frac{\sigma_{YFS}}{\sigma_{BBN}}$
2.0
1.5
1.0
0.5
0
0.2
0.4
0.6
0.8
V
9-88
6029A21

Fig. 5

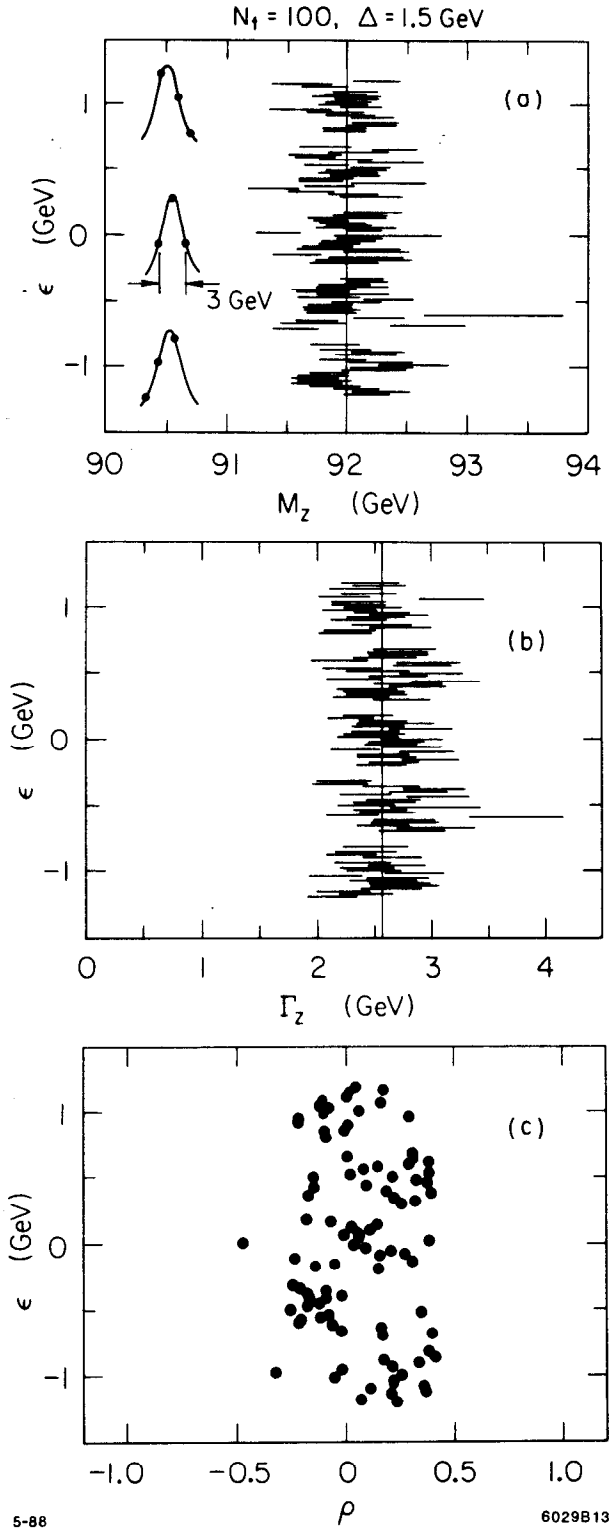

Fig. 6

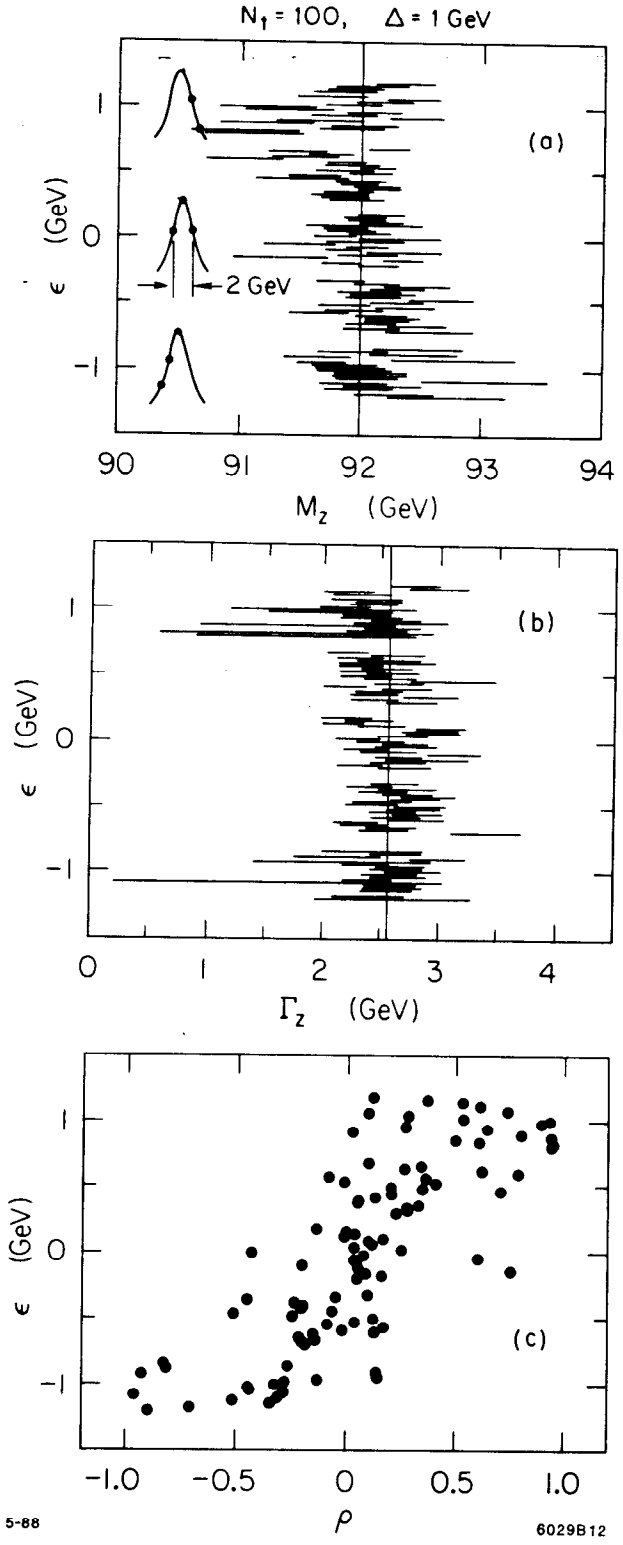

Fig. 7

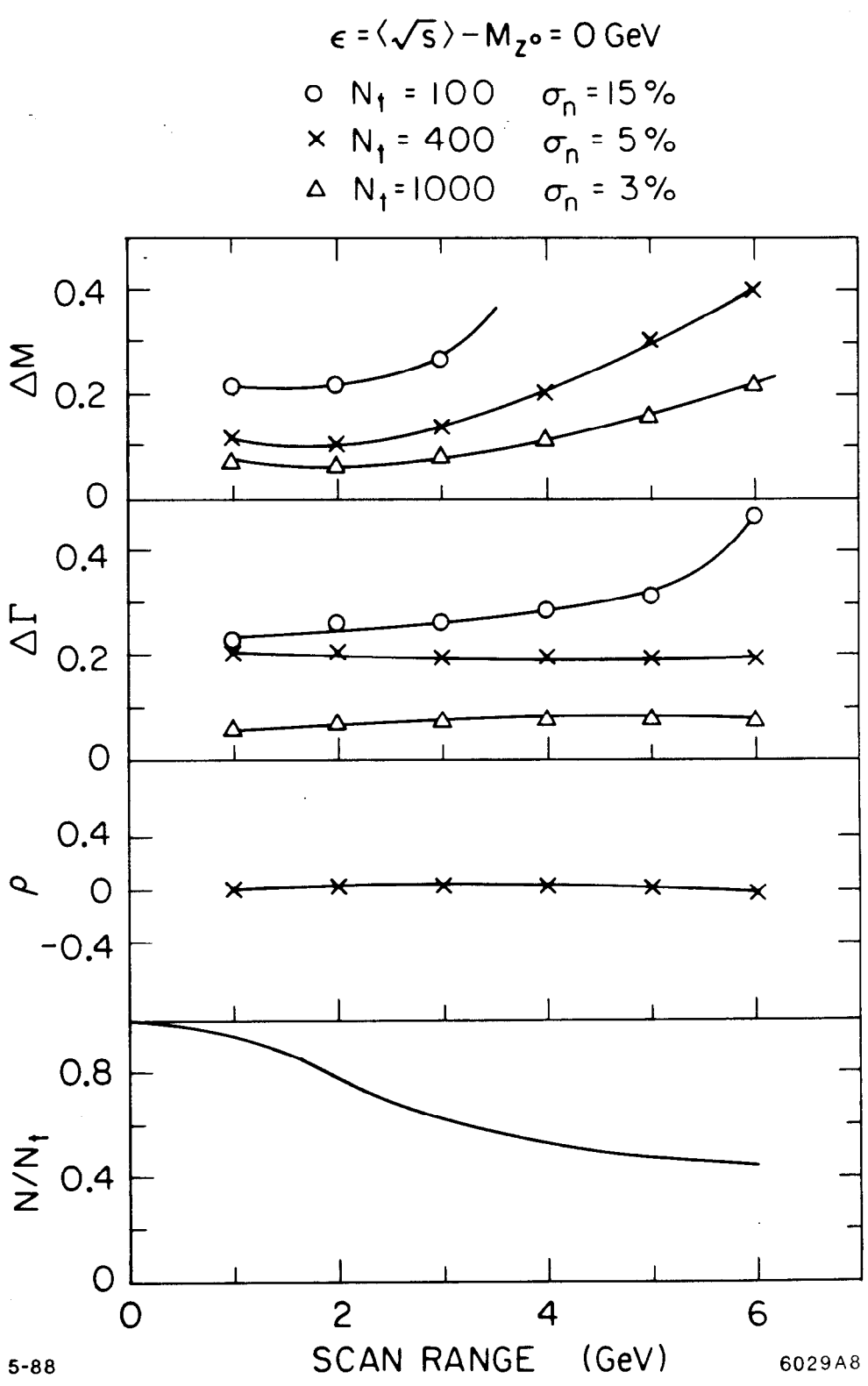
$\epsilon = \langle\sqrt{s}\rangle - M_{Z^0} = 0$ GeV
o $N_t = 100$ $\sigma_n = 15\%$
× $N_t = 400$ $\sigma_n = 5\%$
△ $N_t = 1000$ $\sigma_n = 3\%$
ΔM
ΔΓ
ρ
N/N_t
0.4
0.2
0
-0.4
0.8
2
4
6
SCAN RANGE (GeV)
5-88
6029A8

Fig. 8

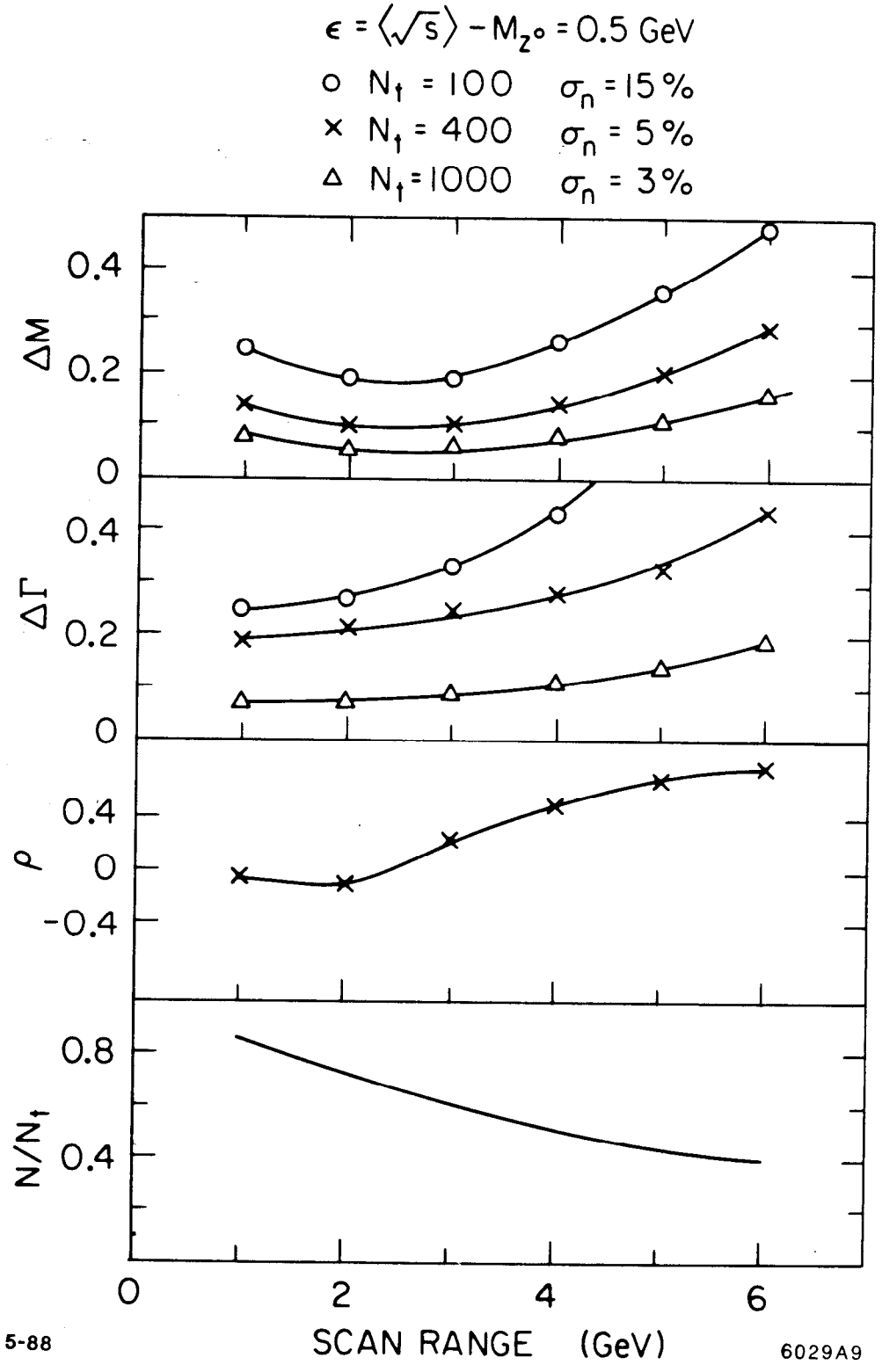
$\epsilon = \langle\sqrt{s}\rangle - M_{Z^0} = 0.5$ GeV
○ $N_t = 100$ $\sigma_n = 15\%$
× $N_t = 400$ $\sigma_n = 5\%$
△ $N_t = 1000$ $\sigma_n = 3\%$
ΔM
ΔΓ
ρ
N/N_t
0.4
0.2
0
-0.4
0.8
0
2
4
6
SCAN RANGE (GeV)
5-88
6029A9

Fig. 9

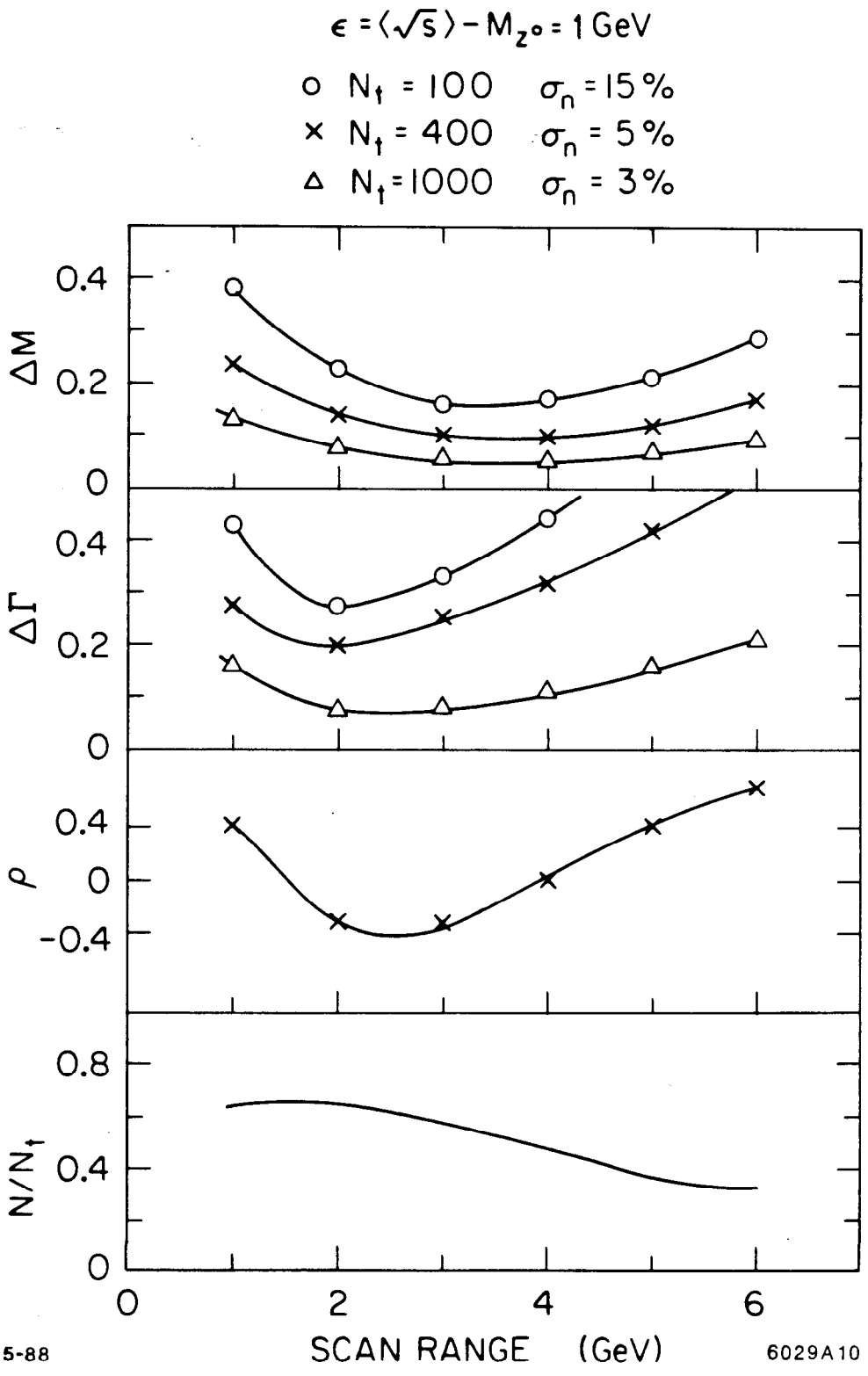
$\epsilon = \langle\sqrt{s}\rangle - M_{Z^0} = 1\,GeV$
o $N_t = 100$ $\sigma_n = 15\%$
× $N_t = 400$ $\sigma_n = 5\%$
△ $N_t = 1000$ $\sigma_n = 3\%$
ΔM
ΔΓ
ρ
N/N_t
0.4
0.2
0
-0.4
0.8
0
2
4
6
SCAN RANGE (GeV)
5-88
6029A10

Fig. 10

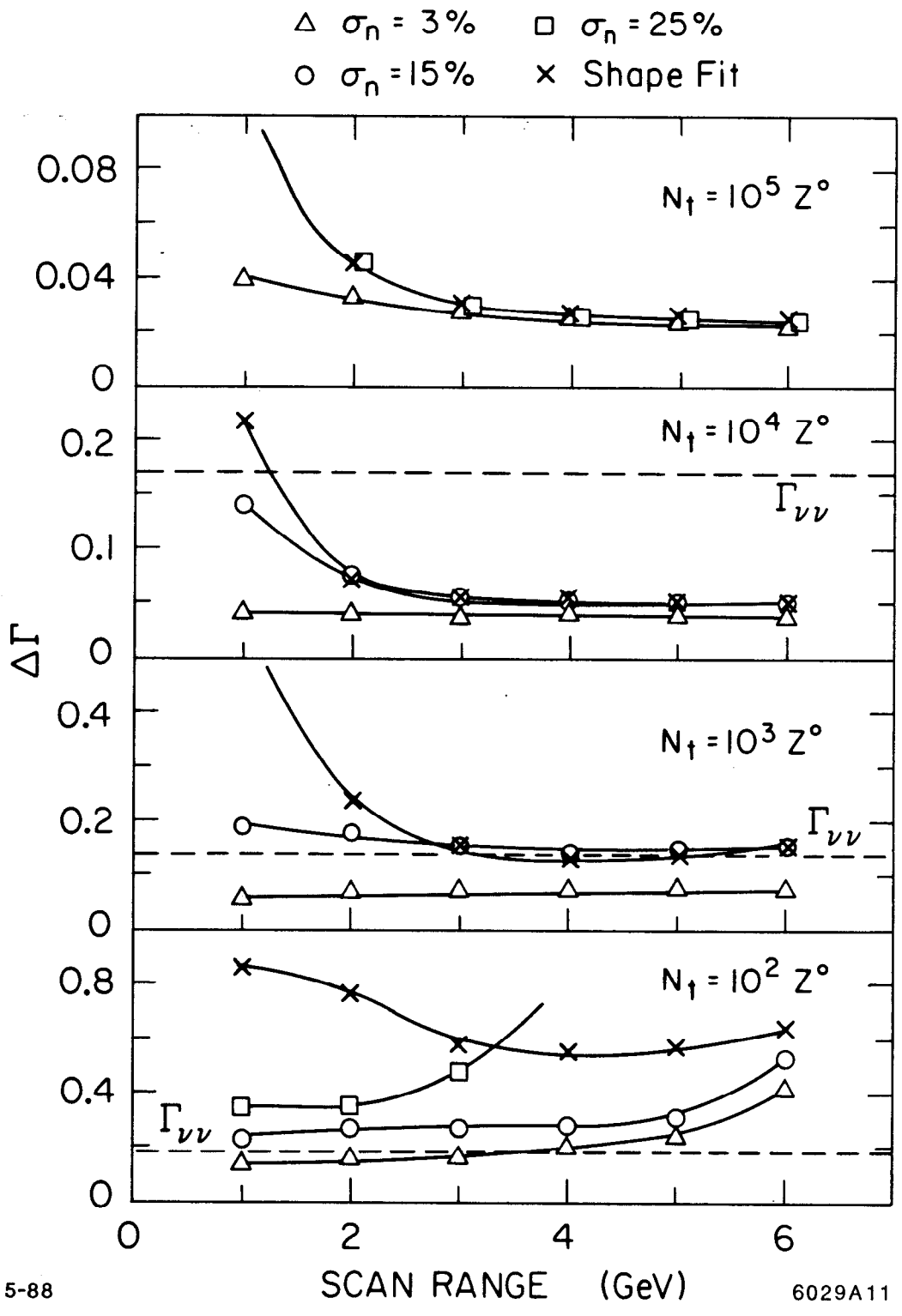
△ σn = 3%
□ σn = 25%
○ σn = 15%
× Shape Fit
0.08
0.04
0
Nf = 10^5 Z°
0.2
0.1
0
Nf = 10^4 Z°
Γνν
ΔΓ
0.4
0.2
0
Nf = 10^3 Z°
Γνν
0.8
0.4
0
Nf = 10^2 Z°
Γνν
0
2
4
6
SCAN RANGE (GeV)
5-88
6029A11

Fig. 11